PHOTOMASK

BACUS—The international technical group of SPIE dedicated to the advancement of photomask technology.

BACUS N • E • W • S

OCTOBER 2015
VOLUME 31, ISSUE 10

EMLC15 Best Paper Award

Experimental validation of novel EUV mask technology to reduce mask 3D effects

Lieve Van Look*, Vicky Philipsen, Eric Hendrickx, imec, Kapeldreef 75, B-3001 Leuven, Belgium

Natalia Davydova, Friso Wittebrood, Robert de Kruif, Anton van Oosten, Junji Miyazaki, Timon Fliervoet, Jan van Schoot, ASML BV, De Run 6501, 5504 DR Veldhoven, The Netherlands

Jens Timo Neumann, Carl Zeiss SMT GmbH, Rudolf-Eber-Str.2, 73447 Oberkochen, Germany

ABSTRACT

Traditional EUV masks, with absorber on top of the multi-layer (ML) mirror, generally suffer from mask 3D effects: H/V shadowing, best focus shifts through pitch and pattern shifts through focus. These effects reduce the overlapping process window, complicate optical proximity correction and generate overlay errors. With further pitch scaling, these mask 3D effects are expected to become stronger, increasing the need for a compensation strategy.

In this study, we have proven by simulations and experiments that alternative mask technologies can lower mask 3D effects and therefore have the potential to improve the imaging of critical EUV layers.

We have performed an experimental imaging study of a prototype etched ML mask, which has recently become available. This prototype alternative mask has only half the ML mirror thickness (20 Mo/Si pairs) and contains no absorber material at all. Instead, the ML mirror is etched away to the substrate at the location of the dark features. For this etched ML mask, we have compared the imaging performance for mask 3D related effects to that of a standard EUV mask, using wafer exposures at 0.33 NA. Experimental data are compared to the simulated predictions and the benefits and drawbacks of such an alternative mask are shown. Besides the imaging performance, we will also discuss the manufacturability challenges related to the etched ML mask technology.

1. Introduction

Mask 3D effects are inherent to EUV lithography, where a large mask topography is combined with non-normal, and asymmetrically distributed incidence angles of the EUV light on the mask.

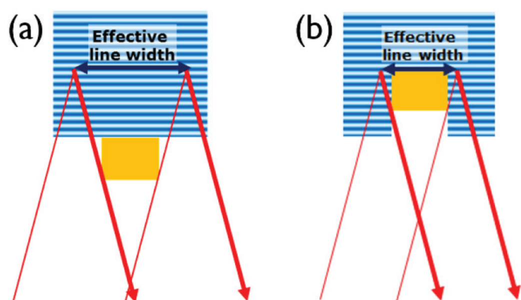

Figure 1. (a) Simplified representation of absorber-induced shadowing, where the effective line width as perceived by the optics is larger than the absorber width. (b) By bringing the absorber closer to the effective reflection plane within the mirror, the effective line width is closer to the absorber width.

TAKE A LOOK INSIDE:

INDUSTRY BRIEFS
—see page 12

CALENDAR
For a list of meetings
—see page 13

SPIE.

9661-19

Editorial

Terra firma, pericolosa or incognita?

Larry Zurbrick, Keysight Technologies, Inc.

Road mapping the technical direction of our industry has been a key element to the planning activities for the equipment/material/software supply chain. As such, the ITRS and the NTRS (National Technology Roadmap for Semiconductors) before it provided the road map framework since first published by the SIA in 1992. The every other year revisions with updates in the intervening years were the “tick tock” of the technology roadmap (to steal a phrase from Intel). This changed in April 2014 when the anticipated 2013 roadmap revision appeared. This was perhaps the last of the “classic More Moore” ITRS Roadmaps since the executive overview announced that more system level drivers and end applications were to be included in future roadmaps and the coming of ITRS 2.0. Justification for the changes currently in progress are based upon the fundamental evolution of the semiconductor industry towards a heterogeneous integration approach to system design. Clearly this is no longer business as usual although it could be argued that business as usual changed more than a decade ago with the advent of equivalent scaling. Is the roadmap turning towards dangerous land (terra pericolosa) or unknown land (terra incognita)?

What does this mean for lithography and mask lithography in particular? Looking at the ITRS 2.0 workshop presentation on More Moore scaling is perhaps not a drastic change in the immediate future for the things that concern those in the equipment/material/software supply chain. Contacted poly pitch, metal pitch and contact CD’s still shrink over the next 5 to 8 years. This means a continuing increase in data volumes, process control and edge placement accuracy as in the past. It appears that we are still on the known lithography roadmap (terra firma) for the immediate future. The red brick walls that appear as roadblocks on our roadmap and how we overcome them provide the continuing challenges and opportunities for innovation in our industry. But then this is yet another story…

N • E • W • S

BACUS News is published monthly by SPIE for BACUS, the international technical group of SPIE dedicated to the advancement of photomask technology.

Managing Editor/Graphics Linda DeLano
Advertising Lara Miles
BACUS Technical Group Manager Pat Wight

■ 2015 BACUS Steering Committee ■

President
Paul W. Ackmann, *GLOBALFOUNDRIES Inc.*

Vice-President
Jim N. Wiley, *ASML US, Inc.*

Secretary
Larry S. Zurbrick, *Keysight Technologies, Inc.*

Newsletter Editor
Artur Balasinski, *Cypress Semiconductor Corp.*

2015 Annual Photomask Conference Chairs
Naoya Hayashi, *Dai Nippon Printing Co., Ltd.*
Bryan S. Kasprowicz, *Photronics, Inc.*

International Chair
Uwe F. W. Behringer, *UBC Microelectronics*

Education Chair
Artur Balasinski, *Cypress Semiconductor Corp.*

Members at Large
Frank E. Abboud, *Intel Corp.*
Paul C. Allen, *Toppan Photomasks, Inc.*
Michael D. Archuletta, *RAVE LLC*
Peter D. Buck, *Mentor Graphics Corp.*
Brian Cha, *Samsung*
Thomas B. Faure, *GLOBALFOUNDRIES Inc.*
Brian J. Grenon, *Grenon Consulting*
Jon Haines, *Micron Technology Inc.*
Mark T. Jee, *HOYA Corp, USA*
Patrick M. Martin, *Applied Materials, Inc.*
M. Warren Montgomery, SUNY, *The College of Nanoscale Science and Engineering*
Wilbert Odisho, *KLA-Tencor Corp.*
Jan Hendrik Peters, *Carl Zeiss SMS GmbH*
Michael T. Postek, *National Institute of Standards and Technology*
Abbas Rastegar, *SEMATECH North*
Douglas J. Resnick, *Canon Nanotechnologies, Inc.*
Thomas Struck, *Infineon Technologies AG*
Bala Thumma, *Synopsys, Inc.*
Jacek K. Tyminski, *Nikon Research Corp. of America (NRCA)*
Michael Watt, *Shin-Etsu MicroSi, Inc.*

SPIE.

P.O. Box 10, Bellingham, WA 98227-0010 USA
Tel: +1 360 676 3290
Fax: +1 360 647 1445
www.SPIE.org
help@spie.org

©2015

All rights reserved.

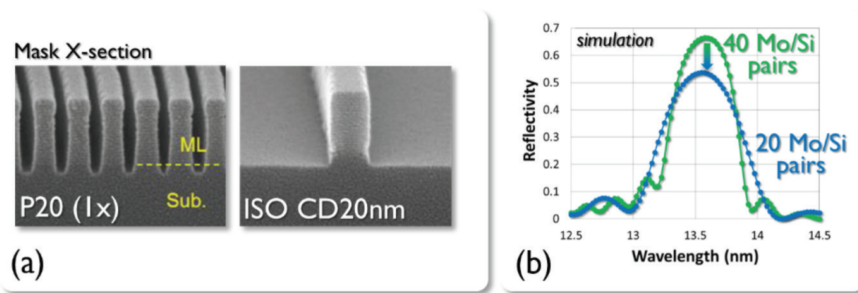

Figure 2. (a) EtchedML20 cross-section SEM images (from [11]), (b) Simulated reflection curves for a Mo/Si ML with 40 and 20 Mo/Si pairs.

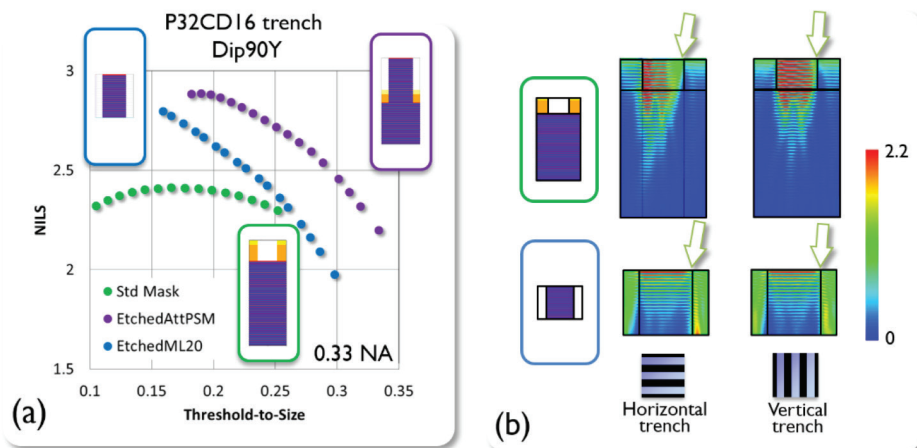

Figure 3. (a) Simulated NILS versus threshold-to-size for printing horizontal dense 16 nm trenches with a standard 70 nm Ta-based absorber mask (green), an EtchedAttPSM (purple) and an EtchedML20 mask (blue). Each dot represents a different mask bias. Illumination condition is a Dip90Y at 0.33 NA. (b) Near-field calculations of the light intensity in the mask for a horizontal and vertical P48 trench at the largest angle occurring when using the Annular source shape of Figure 5.

At the mask side, these effects are noticeable (in simulations or diffractometry experiments[1]) as imbalances within and between the diffraction order amplitudes and phases. On wafer side, mask 3D effects can be easily spotted as H/V printing differences, pattern shifts through focus, and best focus (BF) shifts through pitch. If the balance between the diffraction amplitudes is too distorted, also an Exposure Latitude reduction is seen on wafer. These mask 3D effects are exactly the reason why the use of standard Tabased EUV mask technology at higher NA and 4x magnification was found not to be feasible2, creating the need for the recently proposed anamorphic (4x in X, 8x in Y magnification) EUV optics design for high NA[3]. But also at the current NA of 0.33, imaging performance could certainly benefit from the reduction of mask 3D effects[4].

In literature[5-10] several alternative mask architectures have been proposed that would show less mask 3D effects. In these studies, these alternative masks have been investigated by simulations. From these and our own[4] simulation, the Etched Attenuated Phase Shifting mask (EtchedAttPSM), where the absorber is sunk into the ML mirror (Figure 1(b)), has proven to be a promising candidate to replace the current Ta-based absorber EUV masks. In these simulations, the EtchedAttPSM showed a very high NILS in combination with a low exposure dose. Moreover, mask 3D effects (H/V bias, BF shifts through pitch, pattern shifts through focus) were found to be very small, both at 0.33 and at higher NA's. From the simplified geometrical representation of absorber-induced shadowing in Figure 1, one can understand that bringing the absorber closer to the effective plane of reflection in the ML mirror, as is done in the EtchedAttPSM, can be a way to reduce the mask topography effects.

Even though this mask type shows very promising properties in simulations, with today's technology, it is unfortunately not possible to fabricate a production line-compatible mask where the absorber is placed within the ML. Nevertheless, a great deal of progress has been made in recent years to develop another, related, alternative EUV mask stack. Takai et al. have shown[11] patterning of an etched ML mask with resolution down to a pitch of 20 nm (1x) by using a ML mirror with half of the thickness, being 20 Mo/Si ML pairs. Even though this EtchedML20 mask concept doesn't have any absorber deposited in the etched ML trenches, it is the closest we can get to the Etched Attenuated Phase Shifting mask today. We have therefore opted to concentrate in this work on the so-called EtchedML20 mask, and use it to perform a first experimental validation of the simulated improvement in mask 3D related effects by alternative EUV mask stacks.

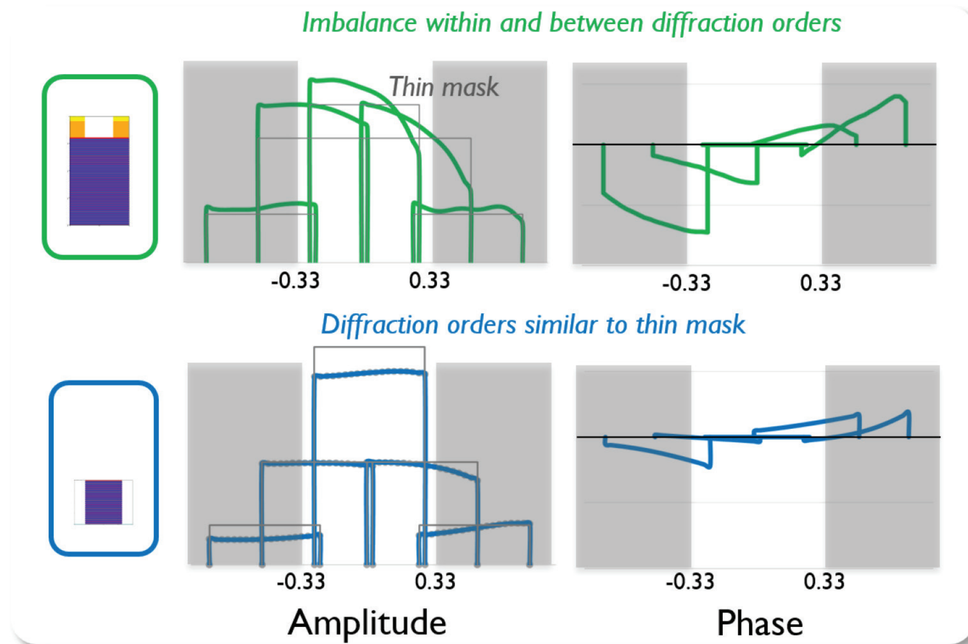

Figure 4. Diffraction amplitudes and phases for a horizontal P48 trench using a standard 70 nm thick Ta-based absorber EUV mask (green) and an EtchedML20 mask (blue). Thin lines indicate the diffraction pattern as obtained from a thin mask calculation.

2. Simulated Benefit of the EdtchedML20

Figure 2(a) shows cross-section SEM images of such an EtchedML20 mask for a dense pitch 20 nm pattern and an isolated feature of 20 nm wide. On this mask, no absorber is present. The dark regions are created by etching away the ML mirror. The isolated ML pattern shown in Figure 2(a), will therefore print to a trench on wafer, when a positive tone resist process is used.

As the mask has 20 Mo/Si ML pairs instead of the usual 40 pairs, the reflectivity is reduced from 63% to 53%. In Figure 2(b), the simulated reflectivity curve through wavelength is shown for the full and the half ML mirror. The mask model used in these simulation is the same as reported by Davydova *et al.*[12]. These simulated values are in agreement with the reported measured data[11]. The reduced reflectivity will result in a higher dose-to-size, or alternatively, a larger mask bias when operating at the same dose as the standard mask.

We compared the simulated NILS through mask CD for the standard mask, the EtchedAttPSM mask and the EtchedML20 mask, all printing 16 nm dense trenches using a Dipole90Y source at an NA of 0.33 (Figure 3(a)). The standard mask shows a sufficiently high NILS, but clearly the EtchedAttPSM mask shows superior printing. This can be read from the graph either as a higher NILS at identical threshold-to-size, or as an identical NILS performance at higher thresholds-to-size (meaning *lower* exposure doses). The EtchedML20 mask is indicated in Figure 3(a) by the blue dots, and simulated NILS performance lies in between the standard mask and the EtchedAttPSM mask, depending on the threshold at which one evaluates the masks.

Simulations indicate that this EtchedML20 mask is also a valuable candidate to consider for reducing mask 3D effects. In Figure 3(b), the near-field images are shown for a vertical and horizontal trench at a pitch of 48 nm (1x). These plots have identical X, Y and color scale and represent the large incidence angle that which will occur when using the Annular setting from Figure 5. We calculate this angle from arcsin($NA/4*\sigma_c$) for the vertical feature, and 6°+arcsin($NA/4*\sigma_c$) for the horizontal feature, where we use 0.8 for σ_c. Let us first consider the case of the standard mask (70 nm Ta-based absorber onto a 40 ML pair mirror, upper images). In the case of a vertical trench on the standard mask, the maximum angle at mask side is 3.8°. Therefore, only a small shadow is cast by the absorber. For the horizontal trench on the standard mask, the maximum angle at mask side has increased to 9.8°, which casts an easily noticeable shadow in the near-field image. This shadow blocks the light from ever reaching the ML mirror, and from contributing to the mask reflection function right above the mask's surface. It is responsible for the H-V printing difference for the standard mask.

For the EtchedML20 mask, the near-field images at the bottom of Figure 3(b) look very different. As no absorber is present on the mask, the EUV light reaches the mirror, regardless of the incoming angle. Hardly any difference can be observed between the near-field images for the two orientations. Consequently, the H-V printing difference is expected to be very small. Interestingly, it seems that a shadow is cast near the bottom of the EtchedML20 mask (left in the nearfield image), and a higher concentration of light is observed at the opposite side of the ML (right in the near-field image) due to reflections from the sidewalls of the ML. These effects seem to have no influence on the imaging as they occur at the mask bottom in regions where reflectivity is zero.

Further evidence of lower mask 3D effects for the EtchedML20 mask can be found in the diffraction pattern simulations. The upper left graph in Figure 4 show the diffraction amplitude for a horizontal pitch 48 trench, imaged with a standard EUV mask (green line).

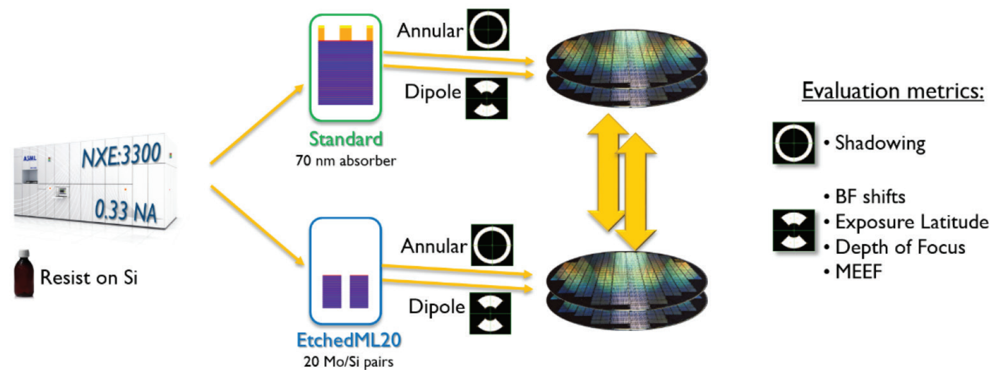

Figure 5. Schematic representation of the experimental set-up followed to achieve an on-wafer comparison of the standard and EtchedML20 mask.

The thin grey line shows the diffraction amplitudes as obtained for the same mask pattern in a thin mask (Kirchhoff) simulation, where mask 3D effects are absent. Any deviation from this Kirchhoff diffraction pattern can be regarded as a manifestation of mask 3D effects. The diffraction pattern for the standard mask shows amplitude imbalances both within the diffraction orders as between the diffraction orders. The same can be said about the diffraction phases (upper right graph). Here, we immediately plot the phase difference with the Kirchhoff phases for easier interpretation of the graphs. For the EtchedML20 mask (blue lines), these imbalances within and between the diffraction order amplitudes and phases are much less pronounced, making the diffraction pattern more similar to the thin mask pattern.

Based on these simulations, we find the EtchedML20 mask a valuable candidate for a first experimental validation of the simulated mask 3D benefit of alternative EUV mask architectures.

3. Experimental Set-up to Validate Simulated Benefit of EtchedML20 at 0.33 NA

In order to validate the simulated performance of the EtchedML20 mask, and more in particular its lower mask 3D effects, we set up the following experiment. We compare the printing performance on wafer of the standard 70 nm Tabased absorber mask and the EtchedML20 proto mask, by exposing near-to-identical wafers with the two masks. We perform back-to-back exposures on the same NXE:3300 scanner, using the same resist process, wafer layout and illumination conditions. Each of the masks contains test line/space patterns with a large variety of pitches and mask trench CDs. The mask is thus the only changing parameter between the two sets of wafers. We have used two illumination conditions: Annular σ0.7-0.9 for investigation of the H/V printing differences, and a Dipole90Y σ0.2–0.9 source shape for all other investigations (BF shifts through pitch, 2Bar CD asymmetry through focus, Process windows, MEEF). Wafers are inspected in center slit using top-down CD-SEM (Hitachi CG5000) and an ASML YieldStar S-200 scatterometer.

Simulations are performed with SLitho-EUV (Synopsys) using the mask stack published by Davydova and co-workers[12].

4. Shadowing Results

On the wafers exposed with the Annular source shape, we have determined the printing difference between two identical features on mask with vertical and horizontal orientation. The measured wafer trench CD through dose of a trench of approximately 22 nm on a pitch of 48 nm, is shown in Figure 6, where the left graph shows the result for the EtchedML20 mask and the right graph that of the standard mask. In order to print to target at similar doses in resist, we have used a positive mask bias on the EtchedML20 mask which is 7 nm larger than on the standard mask. As mentioned above, this was expected due to the reduced reflectivity of this prototype mask.

The H-V printing difference on wafer is more than -3 nm for the standard mask, with the vertical trench printing to a larger CD. For the EtchedML20 mask, both vertical and horizontal trenches print to the same wafer CD.

We have determined the H-V printing difference on wafer for a large range of pitches (Figure 7 (a)). In (b) of the same figure, Aerial Image simulations are shown that reproduce the experimental curve quite accurately. Both in experiment as in the simulations, the H-V printing differences of around -4 nm for the standard mask, are reduced to below 1 nm in the case of the EtchedML20 mask. We attribute the small wiggles in the experimental curve to small mask CD differences between the selected vertical and horizontal mask patterns.

The above results are clear experimental evidence that the shadowing which is responsible for the H/V printing difference in the standard mask, is near to absent in the case of the EtchedML20 mask.

5. Best Focus Shifts Through Pitch Results

Another manifestation of mask 3D effects are Best Focus (BF) shifts through pitch. In the presence of BF shifts through pitch, it is impossible to image all features in the design at their optimum focus in a single print. BF shifts originate from phase errors within and between the diffraction orders[13]. For standard masks, the opaqueness of the absorber, which is directly related to its thickness, plays an important role in the severity of the occurring BF shifts. Thicker absorbers are more opaque and suffer less from BF shifts[14].

We have measured process windows (PWs) through pitch for the standard and the EtchedML20 mask. The wafers used in this comparison are exposed with a Dipole90Y illumination condition and are evaluated at an identical exposure dose of 58 mJ/cm^2. A selection of three PWs through pitch are shown in Figure 8, where a very good PW alignment on the Focus axis is seen for the EtchedML20 mask (left graph), while shifts of slightly more than

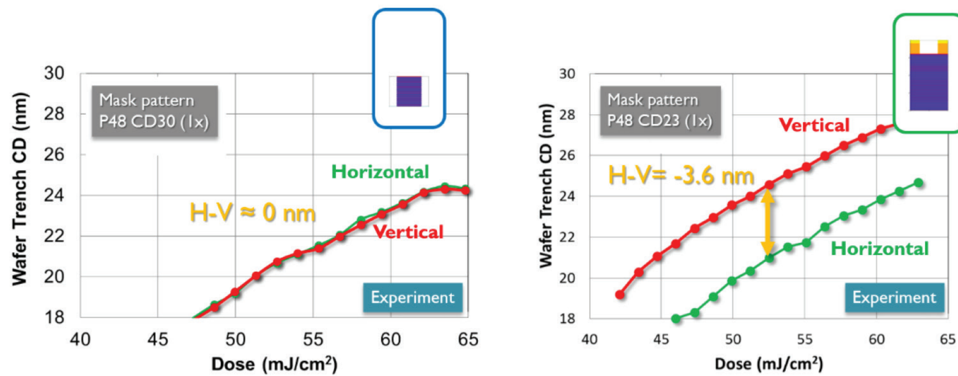

Figure 6. Measured H/V printing difference through dose for a horizontal P48 trench for the EtchedML20 mask (left) and the standard mask (right).

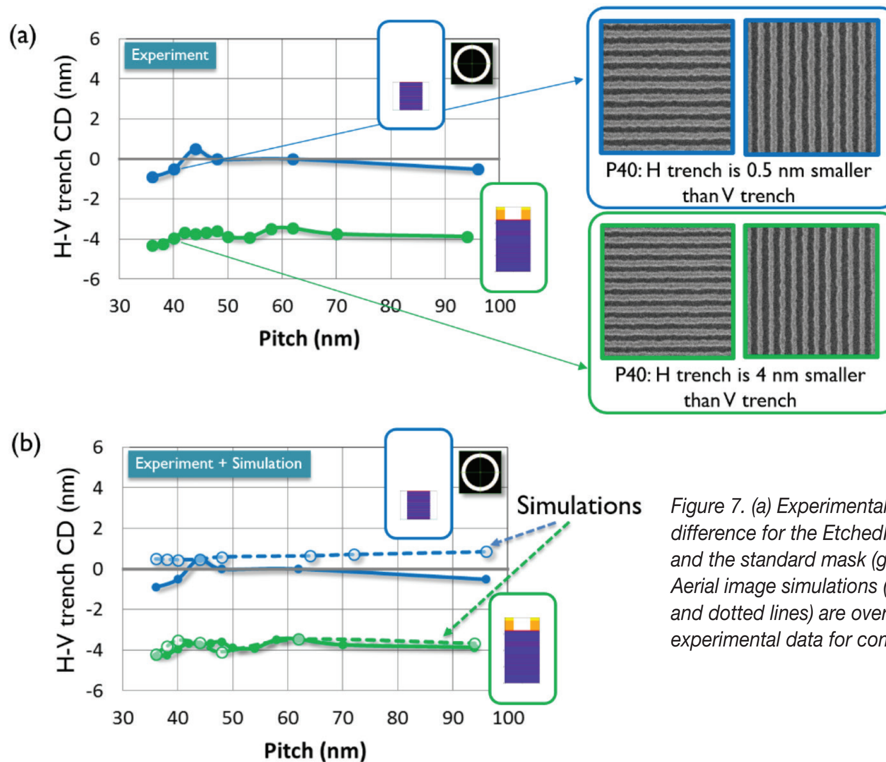

Figure 7. (a) Experimental H-V printing difference for the EtchedML20 (blue) and the standard mask (green). (b) Aerial image simulations (open symbols and dotted lines) are overlaid with the experimental data for comparison.

20 nm are seen for the standard mask (right graph).

We determined the BF shifts through pitch for the two masks using several techniques: a scatterometry-based grating qualification technique[15], and SEM-based CD(focus) and MEEF(focus) curves. The average of all curves as well as the minimum and maximum value detected is plotted in the left panel of Figure 9. Although the curves depend slightly on the detection technique used, all results indicate that the BF shifts for the EtchedML20 mask are smaller than for the standard mask. Moreover, the small BF shift that is still present, has opposite sign compared to the standard mask. Comparing the experimental to the simulated BF shifts in the right-hand side graph of Figure 9, we detect the same two characteristics in the simulated curves. Here, we have determined BF from the Contrast(focus) curve. Simulated BF shifts are clearly smaller for the EtchedML20 mask, and the remaining shifts have the opposite sign compared to the standard mask. Although the absolute value of the BF shifts for the standard mask are larger than what was obtained in the experiments, the trends are very well predicted by the simulations.

6. 2Bar CD Asymmetry Through Focus Results

2Bar patterns are known to be sensitive to aberrations (phase errors). It is therefore no surprise that they are also sensitive to the errors in the amplitudes and phases of the diffraction pattern that are created by the mask 3D effect[16,17]. This makes these pat-

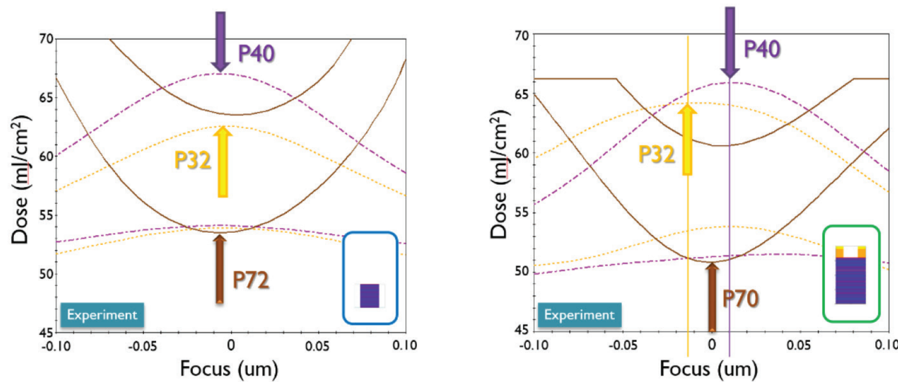

Figure 8. Selected experimental process windows for the EtchedML20 mask (left) and the standard mask (right) showing the absence and presence of best focus shifts, respectively.

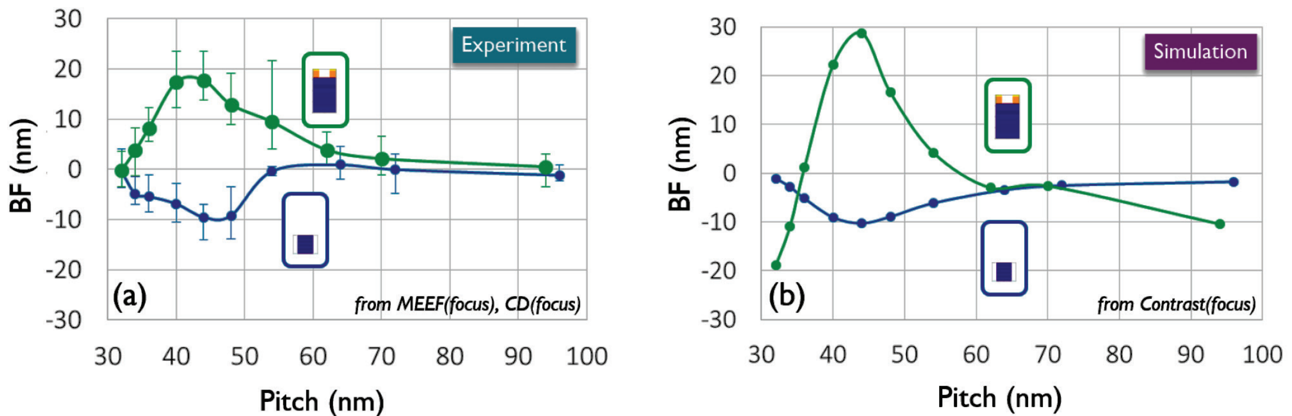

Figure 9. Experimental (left) and simulated (right) Best Focus shifts through pitch for the EtchedML20 (blue) and the standard mask (green).

terns good candidates to be included in our mask comparison. The horizontal 2Bars suffer from a BF difference between the Bossung curves of the two bars, which can also be expressed as a CD asymmetry between the two bars with a linear trend through focus. Vertical 2Bars do not show this effect.

We have compared the 2Bar trench printing performance for the standard and EtchedML20 mask experimentally. An example result can be seen in Figure 10, where the left plot shows the through-focus trend of the CD difference between the lower and upper trench of the 2Bar trench. In this case, the center-to-center distance of the two trenches (small pitch P_S) was designed to be 40 nm, and the pitch between neighboring 2Bar pairs (long pitch P_L) was 400 nm on the standard mask, and 120 nm on the EtchedML20 mask. As is clear from Figure 10, the CD difference through focus for the EtchedML20 mask has a reversed trend compared to the standard mask, and a considerably smaller slope. We compare this experimental result with simulations (right panel of Figure 10), where the trend reversal and the smaller slope for the EtchedML20 mask are clearly reproduced. Moreover, from the comparison of the open (P_L 120 nm) and closed (P_L 400 nm) symbols, it is clear that the long pitch P_L of the 2Bar trench is of minor importance to the observed effect. This leads us to believe that it is justified to compare the 2Bar trenches of the standard and EtchedML20 mask to each other, even though they have different long pitches.

We can summarize the through-focus trend of the 2Bar CD asymmetry by its slope. In Figure 11, we compare these experimental slopes for other horizontal 2Bar trenches with varying small and long pitches. The slope clearly grows with decreasing small pitch for the standard mask, reaching values above 30 nm CD asymmetry per um defocus. For the EtchedML20 mask, all slopes lie below 10 nm/um in absolute value. Note that the small pitch ranges on the two graphs are different: with this Dipole illumination, horizontal 2Bar trenches with the EtchedML20 mask started to resolve at P_S 36 nm, while P_S 32 nm could be reached with the standard mask.

We also verified experimentally that the 2Bar trench CD asymmetry through focus was absent for the vertical 2Bars trenches on both masks. As these wafers were exposed with a DipoleY source shape, the imaging onset in the vertical direction takes place around the 40 nm pitch. Results are shown in Figure 12, where all slopes of the CD left-right asymmetry through focus lie below 5 nm/um, as expected.

7. Process Window Results

We now turn to the PW performance (dose sensitivity, Exposure Latitude and Depth of Focus) of the two masks. Indeed, reduction of mask 3D effects will in the end only be useful when it goes hand in hand with good imaging performance.

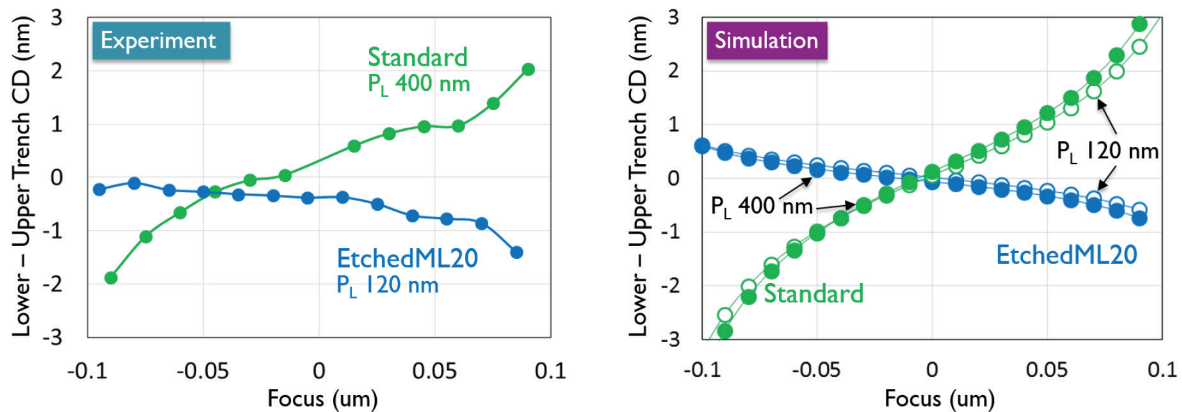

Figure 10. Experimental (left) and simulated (right) 2Bar trench CD asymmetry through focus. The small pitch of the 2Bar is 40 nm in all cases. In the experiment, the long pitch of the 2Bar is 120 nm for the EtchedML20 mask (blue) and 400 nm for the standard mask (green). Simulations are done with both long pitches for both masks.

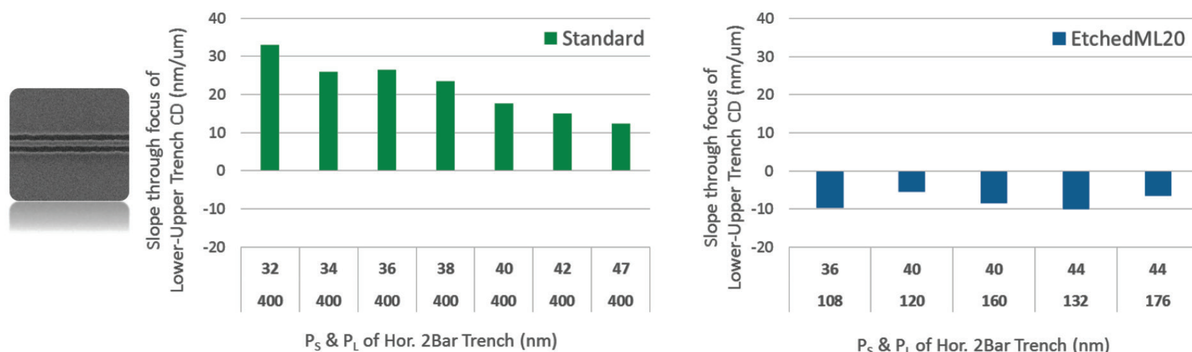

Figure 11. Slope of the horizontal 2Bar trench CD asymmetry through focus for the standard (left) and EtchedML20 mask (right).

We have chosen in this work to evaluate the standard mask and the prototype EtchedML20 mask at the same exposure dose in the resist. This has the consequence that the mask CDs required to print to target on wafer are higher for the EtchedML20 mask. It can be attributed partly to the nature of the etched ML mask itself, and partly due to the use of only half the ML mirror in this prototype mask. Figure 13 shows the experimentally determined mask CDs for the standard (green) and the EtchedML20 mask (blue). The grey dots in the graph indicate the trench wafer target CD, which is 20 nm for pitches higher than 40 nm, and is half-pitch for pitches below 40 nm. Both the amplitude and the range of the mask biases are quite large for the EtchedML20 mask compared to the standard mask.

Using the mask biases as shown in Figure 13, we then determined the dose sensitivity through pitch, the maximal Exposure Latitude (EL) and the Depth of Focus at 8% EL. All these metrics are determined at the same exposure dose of 58 mJ/cm^2. We used a CD specification of 10% of the wafer target, and fitted the PWs using an ellipse. Patterns with insufficient printing quality are excluded from the PW calculation. The PWs are therefore 'process-limited'. The dose sensitivity for the standard (green) and the EtchedML20 mask (blue) is shown in Figure 14. For pitches larger than 60 nm, dose sensitivities are equal for both masks. At lower pitches, ~20% lower dose sensitivity is seen for the standard mask compared to the EtchedML20 mask.

The EL for the standard (green) and EtchedML20 mask (blue), evaluated at the same exposure dose are shown in the left graph of Figure 15. The EL (which is process limited) is lower for the standard mask at the isolated pitches, and about 4% (in absolute values) higher than the EtchedML20 mask at the dense side.

We also determined the Depth of Focus at 8% EL through pitch for the standard (green) and the EtchedML20 mask (blue) (Figure 15, right panel). The reported DoF takes into account process limitations and is found to be lower for the standard mask at the isolated pitches, and very similar for the two masks for pitches below 60 nm.

Overall, for the denser pitches, the standard mask performs better than the prototype EtchedML20 mask. Based on the NILS simulations (see Figure 3(a)), we expect an improvement in the Exposure Latitudes for the EtchedML20 mask when evaluated at a higher dose-to-size (in combination with a smaller mask bias).

Summarizing the Process Window results, the EtchedML20 proto mask already shows decent imaging performance at the same dose as the standard mask, even with half the ML mirror.

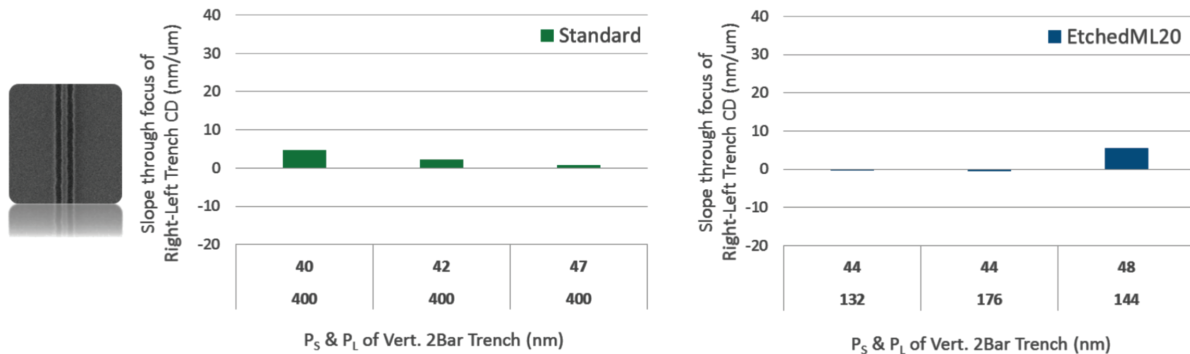

Figure 12. Slope of the vertical 2Bar trench CD asymmetry through focus for the standard (left) and EtchedML20 mask (right).

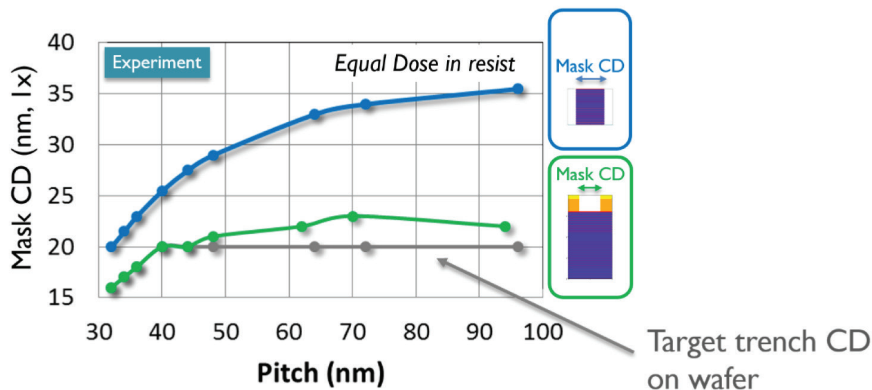

Figure 13. Experimental mask bias required to print the trenches to target (grey) through-pitch at identical exposure dose for the standard (green) and EtchedML20 (blue) mask.

8. MEEF Results

Another metric less related to mask 3D effects, but important from an imaging point of view, is the Mask Error Enhancement Factor (MEEF). The simulated MEEF for the standard and EtchedML20 mask is shown in the right graph of Figure 16. The expected MEEF of the EtchedML20 mask is lower than that of the standard mask. However, looking at the experimentally determined MEEF in the left panel of Figure 16, we notice a steep and unexpected increase of MEEF towards the dense pitches. At the smallest pitch of 32 nm, a MEEF of 4 was recorded. The root cause for this high MEEF is not known today and is the topic of further investigations. Running hypotheses are that the reflectivity of the patterned ML features are less than its physical width or that the ML side walls play a more important role to the imaging as previously assumed.

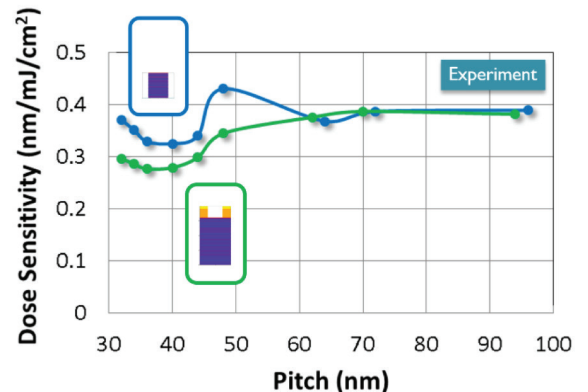

Figure 14. Experimental dose Sensitivity for the EtchedML20 mask (blue) and the standard mask (green).

9. Manufacturability

The EtchedML20 prototype mask has been used in this work to validate the feasibility of reducing mask 3D effect by changing the mask architecture. This prototype mask has served this purpose very well, but it does not represent a manufacturing-ready process. In this section, we list a few of the remaining mask fabrication challenges.

In order to reduce the required mask bias (or equivalently lower the dose-to-size), a higher ML reflectivity, meaning a thicker ML mirror, is required. An increase in the ML thickness will also increase the aspect ratio of the mask features. Avoiding collapse of the patterned ML during cleaning is a challenge. It is also unclear what the impact of the exposed ML mirror sidewalls will be. During the cleaning process, the edges of the ML are prone to damage, both mechanical and chemical. A protection of the sides of the ML patterns is required to ensure the ML reflectivity over the full pattern width, even after multiple cleans.

Another concern is the tapered profile and pitch dependence of

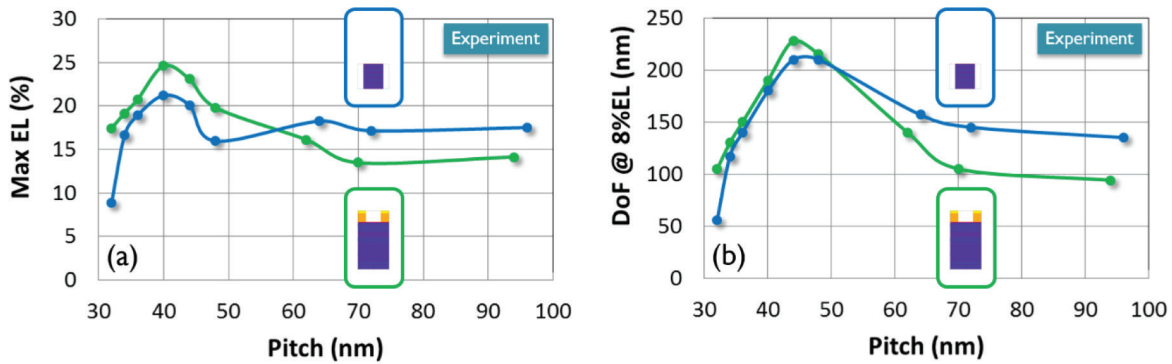

Figure 15. Experimental Exposure Latitude (left) and Depth of Focus at 8% EL (right) through pitch for the EtchedML20 mask (blue) and the standard mask (green). The EL and DoF are calculated by only considering patterns with good printability.

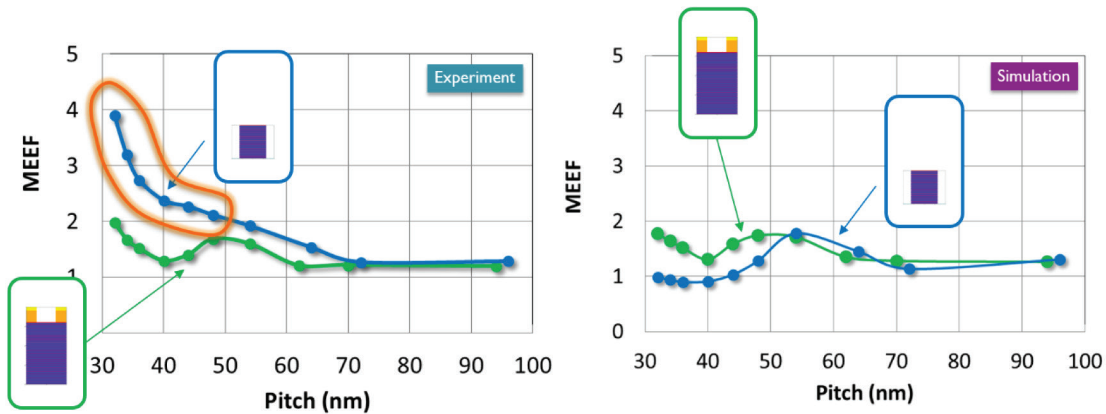

Figure 16. Experimental (left) and simulated (right) MEEF through pitch for the EtchedML20 mask (blue) and the standard mask (green).

the side wall angles that was reported in the cross-section images by Takai *et al.*[11] The effect of the ML sidewall on imaging is not yet assessed, but might be significant. Side wall angle control may therefore be required in the future.

Mask inspection of the patterned etched ML mask introduces new requirements for the mask inspection methods. Simulated inspection results[18] indicate that a Projection Electron Microscope will be able to inspect defects on a patterned etched ML mask down to mask feature aspect ratios of 8.8. No matter what inspection process is deployed, two focal planes will be required to inspect the ML mirror surface and the bottom of the trenches. This could add time and complexity the inspection and review process. The defect challenge will continue with mask repair since replacing missing ML is not possible.

A possible development goal for the etched ML mask is to fill the ML trenches, thus creating a flat top surface on the mask. Our NILS versus threshold simulations for a horizontal 16 nm trench at a pitch of 32 nm (same conditions as in Figure 4(b)) indicate that filling the etched ML trenches with absorber material will give imaging performance similar to the existing EtchedML20 mask. Filling of the etched ML trenches would protect against two of the manufacturability challenges mentioned above: pattern collapse and cleaning durability.

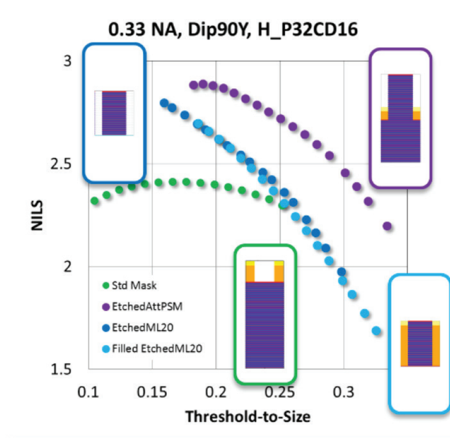

Figure 17. Simulated NILS versus threshold-to-size for printing dense horizontal 16 nm trenches with a standard 70 nm Ta-based absorber mask (green), an EtchedAttPSM (purple), an EtchedML20 mask (dark-blue) and a filled EtchedML20 mask (light-blue). Each dot represents a different mask bias. Illumination condition is a Dip90Y at 0.33 NA.

10. Conclusions

Reducing mask 3D effects by changing the EUV mask architecture has been discussed in literature already for years. Many papers have reported on simulation studies with promising reduction of mask 3D effect (lower shadowing, BF shifts through pitch, pattern shifts through focus). Up to now, no experimental data existed, however, that could confirm these simulations.

In this work, we have performed an experimental comparison at 0.33 NA of a prototype EtchedML20 mask and a standard mask. Wafers were exposed with the two masks under identical conditions and they were inspected for mask3D effects and general imaging performance at the same exposure dose in the resist.

As the most important conclusion from this work, we established that the EtchedML20 prototype mask shows significantly lower mask 3D effects (H/V shadowing, BF shifts through pitch and 2Bar CD asymmetries through focus) compared to the standard mask, in agreement with the simulations.

Secondly, we found the Process Window performance of the prototype EtchedML20 mask to be already quite good, but requiring a high mask bias (in part due to the use of only 20 ML pairs). However, the MEEF for the dense features on the EtchedML mask amounts up to 4 at pitch 32 nm, which is higher than desirable and also higher than expected from simulations. Understanding this high MEEF is a topic of further investigation.

Manufacturability and cleanability of etched ML masks remains a concern today and needs further work. Potentially, filling of the etched ML trenches with absorber or other material can be beneficial for some of the manufacturability challenges.

11. Acknowledgements

We would like to thank Tsukasa Abe, Yasutaka Morikawa, Naoya Hayashi (Dai Nippon Printing), Kosuke Takai, Takashi Kamo (Toshiba) for developing and manufacturing the EtchedML20 mask. We also owe gratitude to Maarten Van Dorst, Peter Rademakers, Laurens de Winter, Thorsten Last (ASML), Greg McIntyre, Rik Jonckheere, Emily Gallagher, Jeroen Van de Kerkhove, Werner Gillijns, Rudi De Ruyter, Vu Luong (imec), Jack Liddle (Zeiss), and Toru Ishizawa (Hitachi Hi-Tech) for valuable input, assistance, discussions, and support.

12. References

[1] Philipsen, V. *et al.*, “Actinic characterization and modeling of the EUV mask stack,” **Proc. SPIE 88860B** (2013).

[2] Neumann, J. T. *et al.*, “Interaction of 3D mask effects and NA in EUV lithography,” **Proc. SPIE 852211** (2012).

[3] Van Schoot, J. *et al.*, “EUV lithography scanner for sub 8 nm resolution,” **Proc. SPIE 94221F** (2015).

[4] Van Look, L. *et al.*, ”Alternative EUV mask technology for Mask 3D effect compensation,” International Symposium on Extreme Ultraviolet Lithography, Washington D.C. (2014).

[5] Deng Y. *et al.*, “Rigorous EM simulation of the influence of the structure of mask patterns on EUVL imaging,” **Proc. SPIE 5037,** 302-313 (2003).

[6] La Fontaine, B. *et al.*, “Architectural Choices for EUV Lithography Masks: Patterned Absorbers and Patterned Reflectors,” **Proc. SPIE 5374,** 300-310 (2004).

[7] Pawloski, A. *et al.*, “Comparative Study of Mask Architectures for EUV Lithography,” **Proc. SPIE 5567,** 762-773 (2004).

[8] Schmoeller, T. *et al.*, “The Impact of Mask Design on EUV Imaging, ” **Proc. SPIE 73792H** (2009).

[9] Takai, K. *et al.*, “Patterning of EUVL binary etched multilayer mask,” **Proc. SPIE 88802M** (2013).

[10] Erdmann, A. *et al.*, “Modeling studies on alternative EUV mask concepts for higher NA,” **Proc. SPIE 86791Q** (2013).

[11] Takai, K. *et al.*, “Capability of etched multilayer EUV mask fabrication,” **Proc. SPIE 923515** (2014).

[12] Davydova, N. *et al.*, “Mask aspects of EUVL imaging at 27nm node and below,” **Proc. SPIE 816624** (2011).

[13] Burkhardt, M. *et al.*, “Best Focus Shift Mechanism for Thick Masks,” **Proc. SPIE 94220X** (2015).

[14] Davydova, N. *et al.*, “Experimental Approach to EUV Imaging Enhancement by Mask Absorber Height Optimization,” **Proc. SPIE 88860A** (2013).

[15] For further details on this technique: henk.niesing@asml.com.

[16] Finders, J. *et al.*, “The impact of mask topography induced phase effects and their mitigation by absorber optimization for ArFi and EUV lithography”, Photomask Japan SPIE Proc. (2015).

[17] De Winter, L. *et al.*, “Understanding the litho impact of phase due to mask effects when using off-axis illumination”, EMLC2015 SPIE Proc. (2015).

[18] Iida, S. *et al.*, “Impact of EUV mask structure on defect detectability of patterned mask inspection using Projection Electron Microscope,” International Symposium on Extreme Ultraviolet Lithography, Washington D.C. (2014).

N • E • W • S

Sponsorship Opportunities

Sign up now for the best sponsorship opportunities

Photomask 2015 —
Contact: Lara Miles, Tel: +1 360 676 3290; laram@spie.org

Advanced Lithography 2016 —
Contact: Lara Miles, Tel: +1 360 676 3290; laram@spie.org

Advertise in the BACUS News!

The BACUS Newsletter is the premier publication serving the photomask industry. For information on how to advertise, contact:

Lara Miles
Tel: +1 360 676 3290
laram@spie.org

BACUS Corporate Members

Acuphase Inc.
American Coating Technologies LLC
AMETEK Precitech, Inc.
Berliner Glas KGaA Herbert Kubatz GmbH & Co.
FUJIFILM Electronic Materials U.S.A., Inc.
Gudeng Precision Industrial Co., Ltd.
Halocarbon Products
HamaTech APE GmbH & Co. KG
Hitachi High Technologies America, Inc.
JEOL USA Inc.
Mentor Graphics Corp.
Molecular Imprints, Inc.
Panavision Federal Systems, LLC
Profilocolore Srl
Raytheon ELCAN Optical Technologies
XYALIS

Industry Briefs

Korean Chipmaker SK Hynix Announces $38bn Investment in 3 New Plants

International Business Times, August 25, 2015

South Korean chipmaker SK Hynix announced plans for three new chip plants in its home country. The world's second biggest memory chip company said it would spend hugely on the project, $38bn in facility investments, which would have updated production techniques to boost its competitiveness in the ever-evolving global semiconductor industry, over the next 10 years.

At a dedication ceremony for a recently completed new chip plant in Icheon, SK Group chairman Chey Tae-Won announced the new plant would get a total of $12.4bn investment, and the remaining amount would be spent on building two more chip factories in Icheon and Cheongju. The new line will be ready for production within the third-quarter, and is expected to produce a maximum 200,000 sheets of 300mm dynamic random-access memory (DRAM) wafers every month. Following the news, shares in SK Hynix jumped as much as 9.3% in South Korea.

SK Hynix's mammoth investment comes as its rivals including Samsung, Micron Technology and Toshiba are taking steps to bolster their production capacity, anticipating high demand for memory chips used in smartphones, tablets and other devices. Due to high demand, the memory chip industry has enjoyed robust profits in recent quarters. SK Hynix reported a 65% on-year increase in second-quarter net profit.

Samsung earlier said it would construct a multi-billion-dollar chip production facility in Pyeongtaek of Seoul to cater to the increasing demand for semiconductors from the smartphone industry. The world's largest memory chipmaker plans to invest $14.7bn in a new plant, which will produce either logic or memory chips. The company is yet to decide on the type of products to be made at the plant.

Equipment Spending Slows but Still Positive in 2015 and 2016

SEMI, September 9, 2015

Front End fab equipment spending (including new, used, and in-house) is projected to increase 5.0 percent in 2015 (to US$ 37.0 billion) and another 6.6 percent in 2016 (to $39.4 billion) according to most recent edition of the SEMI World Fab Forecast. By product segment, foundry is expected to slow in 2015 (-3 percent) but is expected to gain momentum in 2016 (14 percent). In memory, equipment spending is predicted to grow 16 percent by the end of 2015, but will drop about 1 percent in 2016.

Mirroring slow growth in capex and equipment spending, worldwide installed capacity growth is forecasted between 2 and 3 percent in 2015 and 2016. The most added capacity will be seen in foundries (5 percent in 2015 and 4 percent in 2016), Flash including 3D NAND (5 percent in 2015 and 3-4 percent in 2016), and LEDs (14 percent in 2015 and 9 percent in 2016). Capacity additions vary by wafer size with increasing gains in 200mm wafers from 1.6 percent in 2015 to 2.4 percent in 2016 and continuous growth for 300mm wafers with 4 percent each in 2015 and 2016.

According to SEMI's data, at least 23 facilities will begin construction in 4Q15 or later. The SEMI report tracks a total of 43 new and continuous construction projects in 2015 with investment totaling over $5.9 billion.

Equipment Spending (Front End)

in US$ Million | Count of facilities spending

Region	2014	2015	2016	Change 2015	Change 2016	2014	2015	2016
Americas	$ 7,639	$ 5,570	$ 6,932	-27.1%	24.5%	40	43	41
China	$ 4,058	$ 4,198	$ 4,541	3.4%	8.2%	47	50	38
Europe/Mideast	$ 2,182	$ 2,455	$ 2,690	12.5%	9.6%	38	35	35
Japan	$ 4,023	$ 5,363	$ 5,179	33.3%	-3.4%	50	50	45
Korea	$ 7,588	$ 9,141	$ 8,896	20.5%	-2.7%	23	25	25
SE Asia	$ 1,286	$ 1,293	$ 1,462	0.6%	13.1%	19	18	19
Taiwan	$ 8,478	$ 8,995	$ 9,743	6.1%	8.3%	51	49	45
Sum	**$ 35,253**	**$ 37,015**	**$ 39,443**	**5.0%**	**6.6%**	**268**	**270**	**248**

Source: World Fab Forecast report (August 2015) published by SEMI

Mask Supply Chain Preps for 10nm - Technology Generally on Track, but not Everything is Ready

Dylan McGrath on semiengineering.com, September 17th, 2015

As the semiconductor industry gears up for the 10nm logic node—now likely to begin in the second half of 2017—the photomask supply chain is preparing to grapple with the associated challenges, including dramatic increases in photomask complexity, write times and data volumes. The biggest challenges for mask makers at the 10nm node are the addition of triple and quadruple patterning and the growing complexity of the mask features, including curvilinear shapes. Both of these challenges contribute to the overriding problem facing the photomask industry at 10nm and beyond: longer mask write times. Adoption of model-based MDP is widely considered to be critical at the 10nm node, in part because the mask shapes are so small that their proximity to each other has a major impact on the ability to print them on a mask. Smaller feature sizes at the 10nm node also present challenges for mask and reticle inspection tools, which must detect new classes of more minute defects and identify more mask "hotspots." Two areas of the mask supply chain that need to improve before 10nm goes into production are mask materials and repair.

Join the premier professional organization for mask makers and mask users!

About the BACUS Group

Founded in 1980 by a group of chrome blank users wanting a single voice to interact with suppliers, BACUS has grown to become the largest and most widely known forum for the exchange of technical information of interest to photomask and reticle makers. BACUS joined SPIE in January of 1991 to expand the exchange of information with mask makers around the world.

The group sponsors an informative monthly meeting and newsletter, BACUS News. The BACUS annual Photomask Technology Symposium covers photomask technology, photomask processes, lithography, materials and resists, phase shift masks, inspection and repair, metrology, and quality and manufacturing management.

Individual Membership Benefits include:

- Subscription to BACUS News (monthly)
- Eligibility to hold office on BACUS Steering Committee

www.spie.org/bacushome

Corporate Membership Benefits include:

- 3-10 Voting Members in the SPIE General Membership, depending on tier level
- Subscription to BACUS News (monthly)
- One online SPIE Journal Subscription
- Listed as a Corporate Member in the BACUS Monthly Newsletter

www.spie.org/bacushome

Calendar

2015

SPIE Photomask Technology
29 September-1 October 2015
Monterey Marriott and
Monterey Conference Center
Monterey, California, USA
www.spie.org/pm

Co-located with
SPIE Scanning Microscopies
www.spie.org/sg

2016

SPIE Advanced Lithography
San Jose Convention Center
and San Jose Marriott
San Jose, California, USA
www.spie.org/al

Late abstracts will be considered by the chairs. Contact Pat Wight at patw@spie.org

SPIE is the international society for optics and photonics, an educational not-for-profit organization founded in 1955 to advance light-based science and technology. The Society serves nearly 264,000 constituents from approximately 166 countries, offering conferences and their published proceedings, continuing education, books, journals, and the SPIE Digital Library in support of interdisciplinary information exchange, professional networking, and patent precedent. SPIE provided more than $4 million in support of education and outreach programs in 2014. www.spie.org

SPIE.
International Headquarters
P.O. Box 10, Bellingham, WA 98227-0010 USA
Tel: +1 360 676 3290
Fax: +1 360 647 1445
help@spie.org • www.SPIE.org

Shipping Address
1000 20th St., Bellingham, WA 98225-6705 USA

Managed by SPIE Europe
2 Alexandra Gate, Ffordd Pengam, Cardiff,
CF24 2SA, UK
Tel: +44 29 2089 4747
Fax: +44 29 2089 4750
spieeurope@spieeurope.org • www.spieeurope.org

You are invited to submit events of interest for this calendar. Please send to lindad@spie.org; alternatively, email or fax to SPIE.